Available online at www.sciencedirect.com
SCIENCE DIRECT®
Biochimica et Biophysica Acta 1607 (2003) 35–44
BIOCHIMICA ET BIOPHYSICA ACTA
BBA
www.bba-direct.com

Origin of apparent negative cooperativity of F_1-ATPase

Sakurako Ono[a], Kiyotaka Y. Hara[a], Jun Hirao[a], Tadashi Matsui[b], Hiroyuki Noji[c], Masasuke Yoshida[a], Eiro Muneyuki[a,*]

[a] *Chemical Resources Laboratory, Tokyo Institute of Technology, Nagatsuta 4259, Yokohama 226-8503, Japan*
[b] *Department of Biochemistry, Kanazawa Medical University, Uchinada-cho, Ishikawa 920-02, Japan*
[c] *Institute of Industrial Science, University of Tokyo, Tokyo 153-8505, Japan*

Received 27 May 2003; received in revised form 8 August 2003; accepted 11 August 2003

Abstract

In order to get insight into the origin of apparent negative cooperativity observed for F_1-ATPase, we compared ATPase activity and ATPMg binding of mutant subcomplexes of thermophilic F_1-ATPase, $\alpha_{(W463F)3}\beta_{(Y341W)3}\gamma$ and $\alpha_{(K175A/T176A/W463F)3}\beta_{(Y341W)3}\gamma$. For $\alpha_{(W463F)3}\beta_{(Y341W)3}\gamma$, apparent K_m's of ATPase kinetics (4.0 and 233 μM) did not agree with apparent K_m's deduced from fluorescence quenching of the introduced tryptophan residue (on the order of nM, 0.016 and 13 μM). On the other hand, in case of $\alpha_{(K175A/T176A/W463F)3}\beta_{(Y341W)3}\gamma$, which lacks noncatalytic nucleotide binding sites, the apparent K_m of ATPase activity (10 μM) roughly agreed with the highest K_m of fluorescence measurements (27 μM). The results indicate that in case of $\alpha_{(W463F)3}\beta_{(Y341W)3}\gamma$, the activating effect of ATP binding to noncatalytic sites dominates overall ATPase kinetics and the highest apparent K_m of ATPase activity does not represent the ATP binding to a catalytic site. In case of $\alpha_{(K175A/T176A/W463F)3}\beta_{(Y341W)3}\gamma$, the K_m of ATPase activity reflects the ATP binding to a catalytic site due to the lack of noncatalytic sites. The Eadie–Hofstee plot of ATPase reaction by $\alpha_{(K175A/T176A/W463F)3}\beta_{(Y341W)3}\gamma$ was rather linear compared with that of $\alpha_{(W463F)3}\beta_{(Y341W)3}\gamma$, if not perfectly straight, indicating that the apparent negative cooperativity observed for wild-type F_1-ATPase is due to the ATP binding to catalytic sites and noncatalytic sites. Thus, the frequently observed K_m's of 100–300 μM and 1–30 μM range for wild-type F_1-ATPase correspond to ATP binding to a noncatalytic site and catalytic site, respectively.

Keywords: F_1-ATPase; ATP binding; Catalysis; Noncatalytic site; Tryptophan fluorescence

1. Introduction

The F_oF_1-ATP synthase catalyzes ATP synthesis from ADP and phosphate, using the proton-motive force generated by respiratory chain or photosystems. The F_1 region catalyzes synthesis and hydrolysis of ATP in the holoenzyme, but when F_1 is removed from F_o, it catalyzes only ATP hydrolysis. The membrane-embedded part, F_o, consists of at least three kinds of subunits with the stoichiometry ab_2c_{10-14} and works as a proton channel.

Isolated F_1 is water-soluble and consists of five kinds of subunits with the stoichiometry of $\alpha_3\beta_3\gamma\delta\varepsilon$, having six nucleotide binding sites. Three of them are contained mostly within the β subunits and are catalytic sites. The other three sites are contained mostly within the α subunits and they do not have catalytic activity. The crystal structure of mitochondrial F_1-ATPase (MF_1) revealed that α and β subunits are arranged alternately like sections of an orange and that the γ subunit protrudes from the central cavity of $\alpha_3\beta_3$ [1].

Kinetic analyses of the F_1 and F_oF_1-ATP synthase by Boyer's laboratory [2,3] lead to a hypothesis that the three catalytic sites change their nucleotide binding affinity alternately and the γ subunit rotates in the central cavity during the catalysis [4]. This hypothesis was strongly supported by the crystal structure of MF_1 [1] and the rotation of the γ subunit during ATP hydrolysis was directly observed by Noji et al. [5]. However, the precise catalytic mechanism of

Abbreviations: TF_1, soluble ATPase portion of ATP synthase from thermophilic *Bacillus* PS3; MF_1, soluble ATPase portion of mitochondrial ATP synthase; EF_1, soluble ATPase portion of ATP synthase from *Escherichia coli*; Trp mutant, the $\alpha_{(W463F)3}\beta_{(Y341W)3}\gamma$ subcomplex of TF_1; ΔNC mutant, the $\alpha_3\beta_3\gamma$ subcomplex of TF_1 containing two mutations: αK175A/αT176A; CW Less, the $\alpha_3\beta_3\gamma$ subcomplex of TF_1 containing two mutations: αC193S/αW463F; EDTA, ethylenediaminetetraacetic acid; LDAO, lauryl dimethyl aminooxide

* Corresponding author. Tel.: +81-45-924-5232; fax: +81-45-924-5277.
E-mail address: emuneyuk@res.titech.ac.jp (E. Muneyuki).

0005-2728/$ - see front matter © 2003 Elsevier B.V. All rights reserved.
doi:10.1016/j.bbabio.2003.08.006

F_1-ATPase is still unknown. There is a strong cooperativity between three catalytic sites of F_1-ATPase and apparent negative cooperativity observed in ATP hydrolysis was frequently discussed in relation to this cooperativity. However, the relationship between the catalytic activity and catalytic site occupancy has not been figured out and the origin of the apparent negative cooperativity is still unclear. It has been established that when only one site is filled, the catalytic rate is slow (uni-site catalysis) [6,7] and chase-added ATP, as low as 5 μM, accelerates the hydrolysis of the firstly bound ATP [8]. Previously, the apparent negative cooperativity was explained as the rate acceleration by two catalytic sites filling (bi-site catalysis)[1] and three catalytic sites filling (tri-site catalysis)[2] [9]. However, whether the maximal rate of catalysis is attained when all of the three catalytic sites are occupied (tri-site catalysis) or when two of them are occupied (bi-site catalysis) by nucleotides is still a matter of debate [10–16]. In addition, the effect of ADP inhibition and ATP binding to noncatalytic sites should be taken into account for the apparent negative cooperativity.

Weber et al. [15] correlated ATPase activity and nucleotide binding of F_1-ATPase from *Escherichia coli* (EF_1) by introducing a tryptophan residue at catalytic sites. They concluded that the maximal rate of catalysis was attained when all of the three catalytic sites were occupied. According to them, the rate of bi-site catalysis was negligible. ATPase reaction by EF_1 was described with a simple Michaelis–Menten mechanism and ADP inhibition and ATP binding to noncatalytic site did not result in apparent negative cooperativity. Dou et al. [14] also studied the relationship between ATPase activity and nucleotide binding by measuring the fluorescence of tryptophans that had been introduced at catalytic sites of F_1-ATPase from thermophilic *Bacillus* PS3 (TF_1). They also concluded that the maximal rate of catalysis was attained in tri-site catalysis. But the apparent K_m for ATP hydrolysis was higher than the apparent K_m for the third catalytic site filling by ATP as determined by tryptophan fluorescence. Ren and Allison [17] attributed this discrepancy to the effect of ATP binding to noncatalytic sites. They assigned an apparent K_m of some 1–5 μM as the K_m of bi-site catalysis, 40–100 μM as the K_m of tri-site catalysis, and 200–400 μM as the apparent K_m due to ATP binding to noncatalytic site, respectively.

On the other hand, Milgrom et al. [16] studied the ATPase activity of MF_1 and assessed the number of catalytic sites which are occupied by nucleotide when the maximal rate of activity is attained. They found only one apparent K_m (130 μM) which they identified as a K_m of bi-site catalysis and concluded that when only two of the catalytic sites were occupied by nucleotide, the maximal rate of catalysis was attained.

[1] We define bi-site catalysis as a reaction cycle which release product from enzyme species with two catalytic sites filled with nucleotides.

[2] We define tri-site catalysis as a reaction cycle which releases product from enzyme species with three catalytic sites filled with nucleotides.

More importantly, a related question has arisen if the bi-site catalysis is coupled with the rotation of the γ subunit or only tri-site catalysis can drive the rotation. The slow uni-site catalysis may not accompany the rotation of the γ subunit since cross-linking between the γ and β subunits does not inhibit the uni-site catalysis [18]. This contention is supported by the results that the uni-site catalysis was not suppressed when the conformational change of two β subunits was suppressed by cross-linking [19]. As for the bi-site catalysis, Ren and Allison [20] insist that regular rotational motion would not be expected due to the low rate of bi-site catalysis. Yasuda et al. [21] found rotation of the γ subunit at as low as 20 nM ATP. Combined with other kinetic analyses, they conclude that bi-site catalysis is the fundamental mode of rotation and filling all sites does not significantly accelerate, nor add power to, rotation [22], which is in good agreement with Boyer [10–12]. On the other hand, using ITP as a substrate, Weber and Senior [23] reached the conclusion that bi-site hydrolysis activity is negligible, and may not even exist. They argue that only tri-site hydrolysis drives subunit rotation. In order to answer these questions, it is necessary to correlate ATP binding and ATPase activity precisely.

In the present study, we compared mutant subcomplexes of thermophilic F_1-ATPase (TF_1), $\alpha_{(W463F)3}\beta_{(Y341W)3}\gamma$ (Trp mutant) and $\alpha_{(K175A/T176A/W463F)3}\beta_{(Y341W)3}\gamma$ (ΔNC Trp mutant). The Trp mutation which was first introduced by Weber et al. [15] allowed to monitor the nucleotide binding while the ΔNC mutation could eliminate the influence of noncatalytic nucleotide binding sites. Our results indicated that the apparent negative cooperativity observed for wild-type F_1-ATPase in the ATP concentration range between 1 and 2000 μM is due to the ATP binding to catalytic sites and noncatalytic sites. In this concentration range, the frequently observed K_m of 100–300 μM corresponds to ATP binding to a noncatalytic site. The apparent lower K_m of 1–30 μM, which may correspond to the K_m for rotation of the γ subunit observed by Yasuda et al. [22], corresponds to the ATP binding to the third catalytic site, rather than the second catalytic site.

2. Materials and methods

2.1. Strains, plasmids, and proteins

E. coli strain JM109 was used [24] for preparation of plasmids. pKABG1-αW463F was prepared as previously described [25]. The mutation of βY341W was introduced into pTABG1 [25] as previously described [26]. The *Mul*I–*Sma*I fragment of pTABG1 which contained the βY341W mutation was ligated into the corresponding site of pKABG1-αW463F to produce αW463F/βY341W mutant (Trp mutant). The pKABG1-αK175A/αT176A (ΔNC mu-

tation)[3] was prepared as described previously [27]. The *Eco*RI–*Bgl*II fragment which contained the ΔNC mutation was ligated into the corresponding site of pKABG1-αW463F/βY341W to produce ΔNC/Trp mutation. The mutant $\alpha_3\beta_3\gamma$ complexes were purified as previously described [26]. Before the activity measurement, the enzyme was fractionated on a Superdex 200 gel filtration column (Pharmacia Biotech) with a 20 mM 3-morpholinopropanesulfonic acid-KOH (pH 7.0) buffer containing 100 mM KCl for purification. Then, the purified protein was adsorbed on a Butyl-Toyopearl column (TOSOH, Japan). The column was washed with 50 mM Tris–Cl (pH 8.0) buffer, containing 100 mM NaPi, 1 mM ethylenediaminetetraacetic (EDTA), and 20% saturated ammonium sulfate and then with 50 mM Tris–Cl (pH 8.0) buffer containing 1 mM EDTA, 20% saturated ammonium sulfate successively. The protein was eluted with 50 mM Tris–Cl (pH 8.0) buffer containing 1 mM EDTA, for depletion of bound nucleotide. Bound nucleotide was determined using a reverse phase column ODS-80Ts as described in Ref. [28]. After the treatment of nucleotide depletion, bound nucleotide was less than 0.05 mol/mol of $\alpha_3\beta_3\gamma$.

2.2. ATPase activity measurements

ATPase activity was measured at 25 °C in the presence of an ATP-regenerating system in 50 mM Tris–Cl (pH 8.0) buffer containing 100 mM KCl, 3 mM $MgCl_2$, 1 mM EDTA, 50 μg/ml pyruvate kinase, 50 μg/ml lactate dehydrogenase, 2.5 mM phosphoenolpyruvate, 0.2 mM NADH and indicated concentration of ATPMg. Reaction was started by addition of $\alpha_3\beta_3\gamma$. The rate of ATP hydrolysis was determined from the rate of decrease of the absorbance at 340 nm between 3 and 10 s after addition of $\alpha_3\beta_3\gamma$.

2.3. Fluorescence measurements

Fluorescence measurements were performed with FP-777 spectrofluorometer (JASCO, Japan) at 25 °C. After the treatment for nucleotide depletion, $\alpha_3\beta_3\gamma$ in 50 mM Tris–Cl (pH 8.0) buffer containing 1 mM EDTA was diluted to 80–100 nM to a total volume of 1.7 ml in 50 mM Tris–Cl (pH 8.0) buffer 100 mM KCl, 3 mM $MgCl_2$, and 1 mM EDTA. During measurements, the protein solutions were magnetically stirred in the cuvettes. The excitation wavelength was 300 nm. For titration experiments, the emission wavelength was 345 nm. The slit for excitation was set at 1.5 nm and the slit for emission was set at 10 nm. Titrations were carried out by injecting ATPMg solutions into the cuvettes.

[3] In the previous manuscript, we reported that ΔNC mutant contained mutations: αK175A/αT176A/αD261A/αD262A [27]. However, it was recently confirmed that the mutant contained only αK175A/αT176A mutations (Suzuki, T. and Ono, S., unpublished data). In spite of the mistake in the mutated residues, the inability of nucleotide binding to noncatalytic sites remains true judging from the absence of TNP–ATP difference spectrum which appears upon nucleotide binding and the absence of covalent labeling by 2-azido ATP [27].

3. Results

3.1. ATPMg binding and ATPase activity of Trp mutant ($\alpha_{(w463f)3}\beta_{(y341w)3}\gamma$)

In the crystal structure of MF_1, β-Tyr-345 interacts with the adenine moiety of nucleotides bound to the catalytic sites. Weber et al. [15] substituted the equivalent residue in the *E. coli* F_1-ATPase (β-Tyr-331) with tryptophan and estimated the amount of nucleotide bound to catalytic sites fluorometrically. Dou et al. [14] also substituted an equivalent residue in TF_1, β-Tyr-341, with Trp and examined the relationship between nucleotide binding and ATPase activity. In the present study, α-Trp-463 was further substituted with Phe to reduce the background fluorescence. The fluorescence of the β-Trp-341 was reduced by addition of ATPMg with a slight shift of maximal emission wavelength and completely quenched when more than 200 μM ATPMg was added (Fig. 1A). A typical time-course of fluorescence decrease by addition of ATPMg was shown in Fig. 1B. The equilibrium was attained rapidly after addition of ATPMg. Dependencies of fluorescence quenching and ATPase activity on the ATPMg concentration are shown in Fig. 1C.

For evaluation of ATPMg binding curves (Fig. 1C) the following equation was used,

$$\mathrm{FL} = \mathrm{FL}_1 + \mathrm{FL}_2 \times \frac{[\mathrm{MgATP}]}{K_{\mathrm{mF2}} + [\mathrm{MgATP}]} + \mathrm{FL}_3 \times \frac{[\mathrm{MgATP}]}{K_{\mathrm{mF3}} + [\mathrm{MgATP}]} \quad (1)$$

FL_1, FL_2, and FL_3 are the extent of fluorescence decrease that was caused by ATPMg binding to the highest affinity site, second highest affinity site, and the third lowest affinity site, respectively. K_{mF2} and K_{mF3} represent ATPMg binding affinity to the second and third catalytic site. At ATP concentrations lower than that of the enzyme, fluorescence decreased linearly as increasing ATP concentration, indicating a very high affinity (nM order) of the first catalytic site. Thus, K_{mF1}, which represents the ATPMg binding to the first site, was not evaluated. Instead, the contribution of the first site to the fluorescence quenching was treated as a constant value, FL_1, which was determined as the fluorescence decrease when the enzyme concentration and ATP concentration were the same. FL_1 was about one-third of the total fluorescence intensity in the absence of nucleotide, supporting the equal contribution of fluorescence intensity by the three catalytic sites. Estimated parameters are summarized in Table 1.

A clearly downward concave Eadie–Hofstee plot was obtained for the ATPase reaction, (Fig. 1C, inset), indicating apparent negative cooperativity. Therefore, for evaluation of

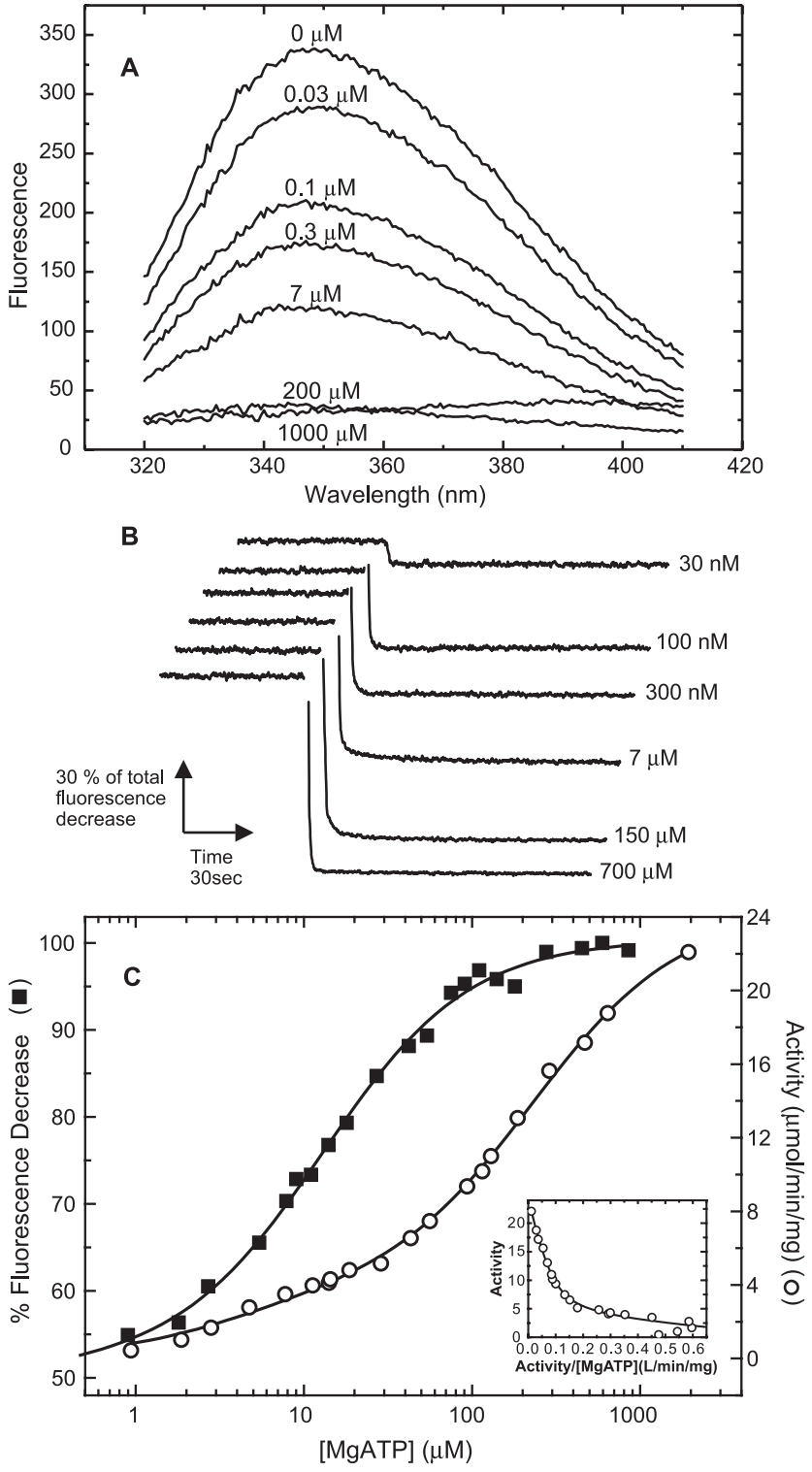

Fig. 1. Comparison of occupancy of the catalytic sites by ATPMg and ATPase activity in Trp mutant. Enzyme concentrations were 80–100 nM for fluorescence measurements and 9–12 nM for ATPase activity measurements. (A) The change in the spectrum of the Trp mutant by the binding of ATPMg. ATPMg concentration for each individual experiment is given in the figure. (B) Time courses for the binding of ATPMg to the Trp mutant. ATPMg solution was added at 60 s after the initiation of the measurement. ATPMg concentration for each individual experiment is given in the figure. (C) The fluorescence decrease and ATPase activity as a function of ATPMg concentration. Filled square, extent of fluorescence decrease which reflects catalytic site occupancy, left-hand scale; open circle, ATPase activity, right-hand scale. ATPase activity was measured with an ATP-regenerating system. The lines are theoretical curves based on the parameters given in Table 1. (Inset, C), Eadie–Hofstee plot of ATPase activity. The line is a theoretical curve using the same parameters.

Table 1
Kinetic parameters deduced from fluorescence titration and ATPase measurement

Trp mutant				
Fluorescence	K_{mF1} (μM)	K_{mF2} (μM)	K_{mF3} (μM)	
	ND[a]	0.016	13	
	(FL_1 = 34.7%)	(FL_2 = 16.7%)	(FL_3 = 51.4%)	
ATPase			K_{mA1} (μM)	K_{mA2} (μM)
			4.0	233
			(V_{max2} = 3.8)	(V_{max3} = 20.5)
ΔNC/Trp mutant				
Fluorescence	K_{mF1} (μM)	K_{mF2} (μM)	K_{mF3} (μM)	
	ND[a]	0.05	26.9	
	(FL_1 = 34.9%)	(FL_2 = 29.8%)	(FL_3 = 35.3%)	
ATPase			K_m (μM)[b]	
			10.0	
			(V_{max2} = 16.6)	
		K_{mA1} (μM)[c]	K_{mA2} (μM)[c]	
		1.3	22	
		(V_{max2} = 4.3)	(V_{max3} = 12.5)	

[a] ND: not determined (nM order).
[b] Parameter deduced by fitting with a linear line.
[c] Parameters deduced by fitting with Eq. (2) guided by eyes. This parameter set is not the best fit which gives minimal χ^2. See text for details.

ATPase activity (Fig. 1C), an equation was used in which two catalytic sites had independent K_m and V_{max} values,[4] as follows.

$$V = V_{max1} \times \frac{[MgATP]}{K_{mA1} + [MgATP]} + V_{max2} \times \frac{[MgATP]}{K_{mA2} + [MgATP]} \quad (2)$$

As there are three catalytic sites, a combination of at least three Michaelis–Menten type reactions may be better than the above equation (Eq. (2)). However, a combination of three Michaelis–Menten type reactions did not give a better fit than Eq. (2) or converge to give a stable parameter set. Therefore, we applied Eq. (2) for phenomenological interpretation.[5] Evaluated parameters are summarized in Table 1.

When we compared the parameters, the K_m values of fluorescence measurement (nM order, 0.016 and 13 μM) and those of ATPase activity measurement (4.0 and 233 μM) did not correspond to each other. The discrepancy is also obvious in Fig. 1C where we tried to overlap the data of fluorescence titration and ATPase activity by adjusting the vertical scale. K_{mF2} determined by the fluorescence measurement was lower than the concentration of the enzyme (80–100 nM) in the solution and should not be regarded as a precise value. With this possible error in K_{mF2} in mind, the K_m values evaluated from the fluorescence measurements in this study were roughly similar to those previously reported by Dou et al. [14] (< 50 nM, 250 nM, and 35 μM). The ATPase parameters also seem to be consistent with the previous results [21]. Actually, the discrepancy between the K_m of fluorescence titration and ATPase reaction was observed in the previous study although it was not quantitatively evaluated. In the previous study, the fluorescence intensities contributed by the three Trp's were assumed to be equal. Here we assumed that the intensities are independent of each other and may not be the same. The converged ratios to the total fluorescence decrease were, FL_1 = 34.7%, FL_2 = 16.7%, and FL_3 = 51.4%, respectively. The discrepancy between the K_m's of fluorescence titration and ATPase activity, unequal fluorescence intensities of the three Trp residues prompted us to consider several possible errors in the measurements and interpretation. For example, there may be some intrinsic difference in the fluorescence intensity of the three tryptophans at the different catalytic sites, or noncatalytic nucleotide binding site on the α subunits might have some influence on the nucleotide binding to catalytic sites.

3.2. ATPMg binding to free-β_{y341w} subunit

To examine the possibility that the fluorescence intensity of the three tryptophans at the different catalytic sites in the absence of nucleotide is significantly different, we further measured the fluorescence of the isolated β subunit which contained a mutation of Tyr-341 to Trp (free-β_{Y341W}). The fluorescence spectrum of free-β_{Y341W} subunit resembled to that of the Trp mutant complex (Fig. 2, inset). The ATPMg and ADPMg concentration dependency of the fluorescence quenching of free-β_{Y341W} is shown in Fig. 2. The K_d's for ATPMg and ADPMg were almost equal, 7.9 μM. The fluorescence intensity of the free-β_{Y341W} was about 37% of the Trp mutant complex, which contains three β subunits. Combined with the results that about one-third of the total fluorescence intensity was quenched when ATP was added to the subcomplex at 1:1 ratio, it is most likely that all of three β-Trp-341 contribute to the total fluorescence in roughly the same manner even if not identical. When the fluorescence was completely quenched, all three catalytic sites are filled with nucleotides. The unequal amplitude of fluorescence quenching, FL_1, FL_2, and FL_3 seems due to some heterogeneity of the $\alpha_3\beta_3\gamma$ complex.

3.3. ATPMg binding and ATPase activity of ΔNC/Trp mutant

The results of fluorescence titration for Trp mutant, especially the significantly unequal values of FL_1, FL_2, and FL_3, suggested some heterogeneity of the enzyme population after addition of ATPMg. For example, it is possible that ATP binding to noncatalytic sites may affect the affinity of the catalytic sites, causing the distorted

[4] The results may be expressed equally by a scheme which includes catalytic site cooperativity [29,30]. But the kinetic parameters deduced by Eq. (2) and the scheme with cooperativity do not differ 10% when the K_m's and V_{max}'s are 10 times different from each other [31].

[5] The K_{mA1} and V_{max1}, K_{mA2} and V_{max2} do not necessarily correspond to the parameters of uni-site catalysis and bi-site catalysis. Rather, the following results suggested that they corresponded to the K_m for tri-site catalysis and ATP binding to noncatalytic site.

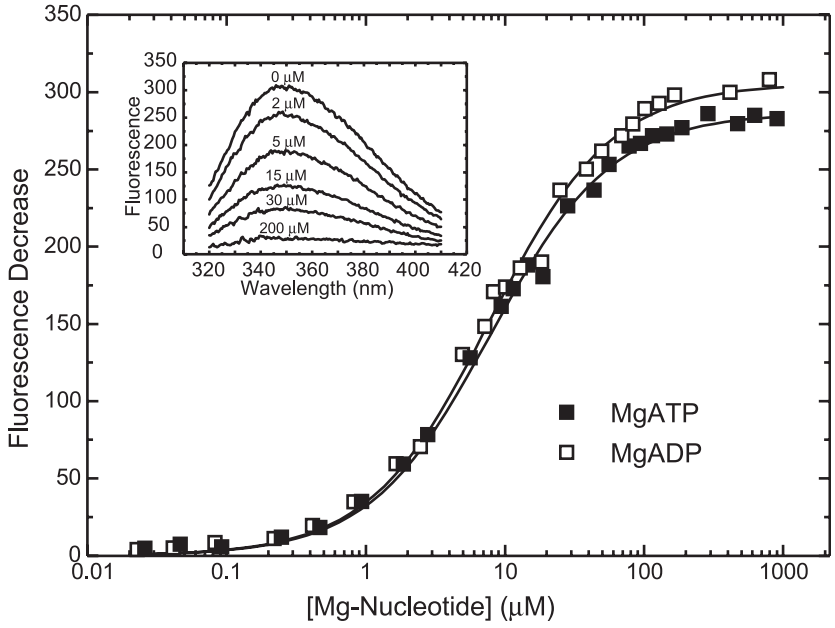

Fig. 2. ATPMg binding to isolated β subunit (free-β_{Y341W}). Protein concentrations were 240–260 nM. Lines are theoretical curves based on K_d values expressed as $FL = FL_t \times ([\text{Mg-Nucleotide}]/(K_d+[\text{Mg-Nucleotide}]))$. Filled square, ATPMg; open square, ADPMg. Inset, spectrum change of free-β_{Y341W} by the binding of ATPMg.

fluorescence titration curve. As for the kinetics of ATPase activity, activation effect of ATP binding to noncatalytic sites may result in an apparent K_m which does not reflect ATP binding to a catalytic site [22,29]. In order to explore the possible effects of noncatalytic sites, we investigated the ATPMg binding and ATPase activity of ΔNC/Trp mutant. The ΔNC mutant is unable to bind nucleotide to noncatalytic sites [27]. ATPMg concentration dependency of ATP binding and ATPase activity is shown in Fig. 3. As in Fig. 1C, we adjusted the vertical scale to fit the data of fluorescence titration to ATPase activity. Fairly good fit between ATPase activity and fluorescence decrease is seen where the latter exceeds 70%, suggesting strong correlation between third ATP binding and ATPase activity.

An Eadie–Hofstee plot of the ATPase activity data (Fig. 3, inset) was rather linear compared with that for Trp mutant

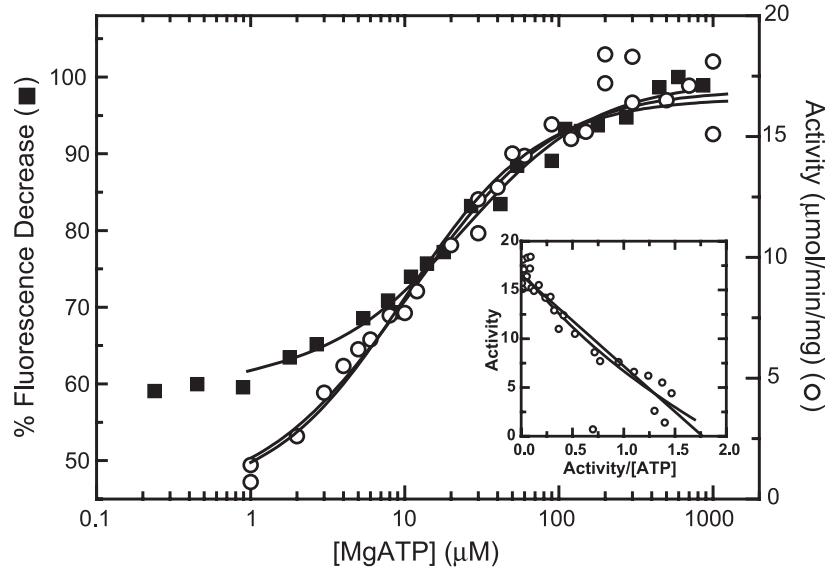

Fig. 3. Catalytic site occupancy and ATPase activity in ΔNC/Trp mutant as a function of ATPMg concentration. Enzyme concentrations were 80–100 nM for fluorescence measurements, and 21–24 nM for ATPase activity measurements. Filled square, extent of fluorescence decrease which reflects catalytic site occupancy, left-hand scale; open circle, ATPase activity, right-hand scale. ATPase activity was measured with an ATP-regenerating system. Lines are theoretical curves based on the parameters given in Table 1. (Inset) Eadie–Hofstee plot of ATPase activity. The lines are theoretical curves using the same parameters.

with noncatalytic sites present (Fig. 1C, inset). When Eq. (2) was used to derive kinetic parameters, K_{mA1} fell into a negative value. A manual adjustment of the kinetic parameters guided by eyes gave a parameter set of $K_{mA1}=1.3$ μM, $K_{mA2}=22$ μM, $V_{max1}=4.3$ U/mg, $V_{max2}=12.5$ U/mg. But application of a single Michaelis–Menten parameter set with a K_m of 10 μM and V_{max} of 16.6 U/mg also gave a fit as good as the others. Therefore, from the kinetic plot, we would not dare to say there is some cooperativity. Actually, the K_{mA1} deduced by manual fitting may be a small blip in the titration curve and may fall well within experimental error. Slight curvature of the linear plot may be a result of time-dependent progress of ADPMg inhibition.

Together with the fluorescence titration, the parameters are summarized in Table 1. The important point is the close coincidence between the K_{mA3} of fluorescence titration (27 μM) and K_m of ATPase activity (22 μM by manual fitting or 10 μM by assuming a simple Michaelis–Menten type dependency). It strongly suggests that when all three catalytic sites are occupied by nucleotides, the maximum activity is attained. Different from the Trp mutant, the fluorescence intensities FL_1, FL_2, and FL_3 were roughly the same for ΔNC/Trp mutant (34.9%, 29.8% and 35.3% of the total fluorescence change, respectively). This may be because the enzyme population was kept homogeneous due to the absence of ATP binding to noncatalytic site.

3.4. k_{off} of ADPMg from Trp mutant under fluorescence measurement condition

K_{mF3} evaluated from the fluorescence measurements of the ΔNC/Trp mutant corresponded to the K_m evaluated from ATPase activity as stated above. As for the Trp mutant, the K_{mA1} of ATPase (4.0 μM) may correspond to the K_{mF3} of fluorescence titration (13 μM) while the K_{mA2} of ATPase reaction (233 μM) corresponds to ATP binding to noncatalytic sites. Then, there seems no counterpart for the K_{mF2} observed in fluorescence titration (0.016 μM for Trp mutant and 0.05 μM for ΔNC/Trp mutant) in the ATPase measurements. Actually, as stated above, the K_{mF2} estimated by fluorescence titration should not be regarded as a precise value because it was below the concentration of the mutant complexes. In addition, there may be some influence of the ADPMg inhibition. When a simple Michaelis–Menten scheme is assumed, K_m is defined as $(k_{off}+k_{cat})/k_{on}$, where k_{on}, k_{off} and k_{cat} are the rate of substrate binding, substrate release, and product release, respectively. When k_{cat} was decreased by an inhibition, the K_m apparently decreases. By analogy, the K_m estimated in fluorescence titration may be an underestimate of the real value. In particular, at μM concentrations of ATPMg, most of the ATPMg was hydrolyzed quickly and most of the enzyme complex may have fallen into ADPMg-inhibited state. The ADPMg-inhibited enzyme tightly retains nucleotides, resulting in an apparently low bi-site K_{mF2}. If this is the case, k_{off} of ADP from the enzyme under the fluorescence measurement conditions is expected to be significantly smaller than the ATPase turnover rate.

To examine the possibility that the K_{mF2} for the second catalytic site was underestimated in the fluorescence measurement due to ADPMg inhibition, the k_{off} of ADP was measured by trapping ADP released from Trp mutant using a cysteine- and tryptophan-less mutant $\alpha_3\beta_3\gamma$ (CW Less) [25] (Fig. 4). Upon addition of the CW Less mutant, fluorescence was recovered. After subtraction of the baseline shift upon the addition of the CW Less mutant, there was a slow recovery of the fluorescence following a rapid increase. The rate calculated from the slow phase was about 0.01 s^{-1} (ADPMg concentration at 100 and 300 nM). If we apply the k_{on} for ATP, evaluated from a single molecule experiment (2.7×10^7 M^{-1} s^{-1} [21]), and k_{off} for ATP is assumed to be the same order of magnitude as the k_{off} for ADP described above, the apparent K_m will be on the order of 10^{-10} M. This may qualitatively account for the very low K_m of the second catalytic site evaluated from the fluorescence measurements.

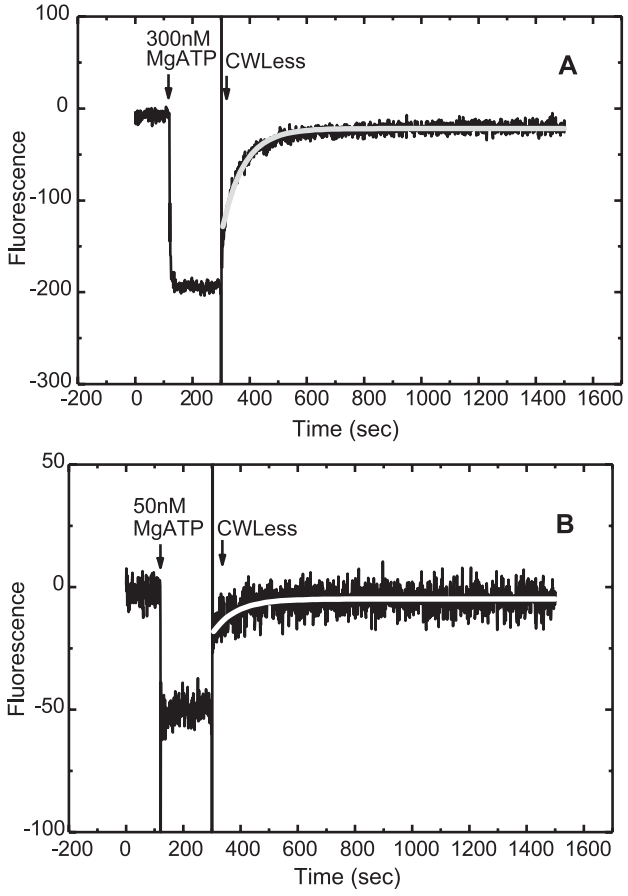

Fig. 4. Time course for the release of ADPMg from Trp mutant. The concentration of Trp mutant was about 100 nM. ATPMg solution was added at 120 s after the initiation of measurement. CW Less (about 1 μM) was added at 300 s. The theoretical lines for the time course were calculated assuming an exponential increase of the fluorescence intensity. The change in fluorescence intensity by injection of CW Less solution was subtracted.

4. Discussion

The kinetics of F_oF_1, F_1, and its subcomplexes are complicated due to the presence of strong cooperativity between catalytic sites, ADPMg inhibition, ATP binding to noncatalytic sites, and so on. In the present study, the results and explanations are fairly consistent with those reported by Ren and Allison [17]. They compared steady state ATPase reaction and fluorescence titration in the presence or absence of lauryl dimethyl aminooxide (LDAO). In the absence of LDAO, they assigned three K_m's of ATP hydrolysis which corresponded to bi-site catalysis, tri-site catalysis and activation by ATP binding to noncatalytic sites by linear extrapolations of Lineweaver–Burk plots. However, fluorescence titration gave a complex curve and could not give a reliable K_m of the bi-site catalysis as was the case in our present study. They attributed this anomaly to an equilibrium between active enzyme complex and ADPMg-inhibited complex. Actually, in the presence of LDAO, which shifts the equilibrium to the active complex, the fluorescence titration curve gave a K_m of bi-site catalysis (0.9 μM) which agreed fairly well with the K_m of ATPase activity (ca. 3–5 μM). In the present study, we avoided the influence of noncatalytic sites by using ΔNC/Trp mutant. In case of ΔNC/Trp mutant, the equilibrium between the active and ADP-inhibited complex was shifted towards ADPMg-inhibited form and resultant fluorescence titration curve gave three phases which correspond to uni-site, bi-site, and tri-site occupancy with approximately the same fluorescence intensity.

Our results of fluorescence titration indicated that for the ΔNC/Trp mutant (and also Trp mutant), the K_m for the uni-site catalysis is at most in 10 nM range, K_m for bi-site catalysis in 10–50 nM, and the K_m for the tri-site catalysis is ca. 10–30 μM. Comparison of the steady state ATPase kinetics of ΔNC/Trp mutant and Trp mutant strongly suggested that the apparent K_m of 100 μM or higher (K_{mA2}) observed for Trp mutant (and wild-type enzyme) represents ATP binding to noncatalytic sites and tri-site K_m of fluorescence titration (K_{mF3}) corresponds to the K_{mA1} of ATPase reaction. The analysis of ATPase activity, however, did not give a clear counterpart to the K_{mF2} (bi-site catalysis) in fluorescence titration. In this case, the absence of an apparent K_m of bi-site catalysis in ATPase measurements which should correspond to the K_{mF2} determined from fluorescence titration may be attributed to the severe inhibition by ADPMg for the latter condition and difficulty in resolving multiple K_m's from ATPase kinetics. Actually, the K_{mF2} determined from fluorescence titration might be an underestimate. The absence of an ATP-regenerating system and ATPase concentration higher than that in ATPase measurement should accumulate significant concentration of ADP under the conditions of fluorescence titration, which in turn causes inhibitory strong binding of ADP to the catalytic sites. The retarded release of ADP was indeed clearly shown using the trapping by CW Less mutant. As for the ATPase kinetics, it is sometimes quite difficult to resolve multiple K_m's from a subtle curvature of the kinetic plots. Even in the presence of an ATP-regenerating system, ATPase activity at low ATP concentrations may be underestimated due to ADPMg inhibition. This may cause significant underestimation of the contribution of bi-site catalysis to the total activity. Or, it is possible that the K_m for the bi-site catalysis is really low even in the absence of ADPMg inhibition and V_{max} accompanying the K_m is very low. In case of V_1-ATPase from *Thermus thermophilus* which is closely related to F-type ATPase but lacks noncatalytic sites, an Eadie–Hofstee plot of ATPase gave a straight line [30]. Anyway, the absence of a clear negative cooperativity in ΔNC/Trp mutant and its presence in Trp mutant lead to a conclusion that the apparent negative cooperativity observed in μM to mM range of ATP arises mostly from the ATP binding to noncatalytic site which activates the ADPMg-inhibited form of the enzyme. Our results suggest that the cooperativity between catalytic sites does not contribute much to the negative cooperativity experimentally observed in μM to mM range of ATP.

Our present results strongly indicate that the appearance of the major ATPase activity is correlated with the filling of the third catalytic site. The so-called bi-site catalysis does not seem to have much contribution to the overall ATPase activity. Actually, Weber and Senior [23,31] insist that bi-site catalysis has little turnover rate and is not coupled with rotation of the central γ subunit. But there is much controversy on this point. Ren and Allison [17,20] assigned some catalytic activity to the bi-site mode, but they regarded tri-site activity as the normal activity which is coupled with the rotation of γ subunit and made a model based on the tri-site catalysis. On the other hand, Yasuda et al. [22] observed rotation using a small gold particle as a marker at as low as 20 nM ATP and concluded that the rotation was driven by bi-site catalysis. But their K_m for the rotation was about 15 μM. Compared with the binding data of fluorescent titration here, they might have been observing rotations driven by tri-site catalysis. Milgrom et al. [16] carefully examined the ATPase kinetics of MF_1 and found a single K_m of 130 μM for MF_1. They assigned the K_m as that of bi-site catalysis and concluded that maximum ATPase activity is attained when two catalytic sites were filled. Zhou and Boyer [32] examined the ATP synthesis by membrane bound CF_oF_1 and concluded that maximum ATP synthesis occurs when two catalytic sites were filled with nucleotides. Boyer [13] recently admitted that three catalytic sites may be filled with nucleotides, but insists that the bi-site catalysis is the essential mode of the enzyme and filling a third catalytic site at most modulates the activity of the enzyme to some extent. He also pointed out many reasonable difficulties in measuring nucleotide binding by Trp fluorescence. It seems that the presently most important point is whether bi-site catalysis is coupled with the rotation of the γ subunit while tri-site activity has only an accessory role or bi-site catalysis

is so slow and the rotation of the γ subunit is exclusively driven by tri-site catalysis. Our present study did not give a clear evidence for a possible role of the bi-site cycle but cannot exclude the possibility that bi-site catalysis is coupled with the rotation of the γ subunit. Obviously, further careful study is required.

Our present conclusion is slightly different from our previous report [27]. In our previous study, K_m of ΔNC mutant was determined to be 135 μM, which was smaller than that of the wild-type enzyme (187 μM). We previously ignored the difference and concluded that the apparent K_m of ATP hydrolysis (187 μM for wild-type enzyme) really represents ATP binding to a catalytic site [27,33]. The additional data on ATP binding measured by Trp fluorescence led us to the present conclusion with greater confidence.

Acknowledgements

We thank our colleagues, Dr. Y. Kato-Yamada, Dr. T. Suzuki, and Dr. T. Hisabori for their helpful discussions, as well as Dr. J. Hardy for her careful reading of the manuscript.

References

[1] J.P. Abrahams, A.G. Leslie, R. Lutter, J.E. Walker, Structure at 2.8 Å resolution of F_1-ATPase from bovine heart mitochondria, Nature 370 (1994) 621–628.
[2] P.D. Boyer, A perspective of the binding change mechanism for ATP synthesis, FASEB J. 3 (1989) 2164–2178.
[3] P.D. Boyer, The binding change mechanism for ATP synthase. Some probabilities and possibilities, Biochim. Biophys. Acta, (1993) 215–250.
[4] M.J. Gresser, J.A. Myers, P.D. Boyer, Catalytic site cooperativity of beef heart mitochondrial F_1 adenosine triphosphatase. Correlations of initial velocity, bound intermediate, and oxygen exchange measurements with an alternating three-site model, J. Biol. Chem. 257 (1982) 12030–12038.
[5] H. Noji, R. Yasuda, M. Yoshida, K.J. Kinosita, Direct observation of the rotation of F_1-ATPase, Nature 386 (1997) 299–302.
[6] C. Grubmeyer, R.L. Cross, H.S. Penefsky, Mechanism of ATP hydrolysis by beef heart mitochondrial ATPase. Rate constants for elementary steps in catalysis at a single site, J. Biol. Chem. 257 (1982) 12092–12100.
[7] D. Cunningham, R.L. Cross, Catalytic site occupancy during ATP hydrolysis by MF_1-ATPase. Evidence for alternating high affinity sites during steady-state turnover, J. Biol. Chem. 263 (1988) 18850–18856.
[8] H.S. Penefsky, Rate of chase-promoted hydrolysis of ATP in the high affinity catalytic site of beef heart mitochondrial ATPase, J. Biol. Chem. 263 (1988) 6020–6022.
[9] R.L. Cross, C. Grubmeyer, H.S. Penefsky, Mechanism of ATP hydrolysis by beef heart mitochondrial ATPase rate enhancements, J. Biol. Chem. 257 (1982) 12101–12105.
[10] P.D. Boyer, ATP synthase—past and future, Biochim. Biophys. Acta 1365 (1998) 3–9.
[11] P.D. Boyer, Catalytic site forms and controls in ATP synthase catalysis, Biochim. Biophys. Acta 1458 (2000) 252–262.
[12] P.D. Boyer, Toward an adequate scheme for the ATP synthase catalysis, Biokhimiya 66 (2001) 1058–1066.
[13] P.D. Boyer, Catalytic site occupancy during ATP synthase catalysis, FEBS Lett. 512 (2002) 29–32.
[14] C. Dou, P.A.G. Fortes, W.S. Allison, The $\alpha_3(\beta Y341W)_3$ γ subcomplex of the F_1-ATPase from the thermophilic *Bacillus* PS3 fails to dissociate ADP when MgATP is hydrolyzed at a single catalytic site and attains maximal velocity when three catalytic sites are saturated with MgATP, Biochemistry 37 (1998) 16757–16764.
[15] J. Weber, S. Wilke-Mounts, R.S.F. Lee, E. Grell, A.E. Senior, Specific placement of tryptophane in the catalytic sites of *Escherichia coli* F_1-ATPase provides a direct probe of nucleotide binding: maximal ATP hydrolysis occurs with three sites occupied, J. Biol. Chem. 268 (1993) 20126–20133.
[16] Y.M. Milgrom, M.B. Murataliev, P.D. Boyer, Bi-site activation occurs with native and nucleotide-depleted mitochondrial F_1-ATPase, Biochem. J. 330 (1998) 1037–1043.
[17] H. Ren, W.S. Allison, Substitution of βGlu_{201} in the $\alpha_3\beta_3\gamma$ subcomplex of the F_1-ATPase from the thermophilic *Bacillus* PS3 increases the affinity of catalytic sites for nucleotides, J. Biol. Chem. 275 (2000) 10057–10063.
[18] J.J. Garcia, R.A. Capaldi, Unisite catalysis without rotation of the γ–ε domain in *Escherichia coli* F_1-ATPase, J. Biol. Chem. 273 (1998) 15940–15945.
[19] S.P. Tsunoda, E. Muneyuki, T. Amano, M. Yoshida, H. Noji, Cross-linking of two β subunits in the closed conformation in F_1-ATPase, J. Biol. Chem. 274 (1999) 5701–5706.
[20] H. Ren, W.S. Allison, On what makes the γ subunit spin during ATP hydrolysis by F_1, Biochim. Biophys. Acta 1458 (2000) 221–233.
[21] R. Yasuda, H. Noji, K.J. Kinosita, M. Yoshida, F_1-ATPase is a highly efficient molecular motor that rotates with discrete 120° steps, Cell 93 (1998) 1117–1124.
[22] R. Yasuda, H. Noji, M. Yoshida, K. Kinosita Jr., H. Itoh, Resolution of distinct rotational substeps by submillisecond kinetic analysis of F_1-ATPase, Nature 410 (2001) 898–904.
[23] J. Weber, A.E. Senior, Bi-site catalysis in F_1-ATPase: does it exist? J. Biol. Chem. 276 (2001) 35422–35428.
[24] C. Yanisch-Perron, J. Vieira, J. Messing, Improved M13 phage cloning vectors and host strains: nucleotide sequences of the M13mp18 and pUC19 vectors, Gene 33 (1985) 103–119.
[25] T. Matsui, M. Yoshida, Expression of the wild-type and the Cys-/Trp-less $\alpha_3\beta_3\gamma$ complex of thermophilic F_1-ATPase in *Escherichia coli*, Biochim. Biophys. Acta 1231 (1995) 139–146.
[26] C. Dou, N.B. Grodsky, T. Matsui, M. Yoshida, W.S. Allison, ADP-fluoroaluminate complexes are formed cooperatively at two catalytic sites of wild-type and mutant $\alpha_3\beta_3\gamma$ subcomplexes of the F_1-ATPase from the thermophilic *Bacillus* PS3, Biochemistry 36 (1997) 3719–3727.
[27] T. Matsui, E. Muneyuki, M. Honda, W.S. Allison, C. Dou, M. Yoshida, Catalytic activity of the $\alpha_3\beta_3\gamma$ complex of F_1-ATPase without noncatalytic nucleotide binding site, J. Biol. Chem. 272 (1997) 8215–8221.
[28] T. Hisabori, E. Muneyuki, M. Odaka, K. Yokoyama, K. Mochizuki, M. Yoshida, Single site hydrolysis of 2′,3′-*O*-(2,4,6-trinitrophenyl)-ATP by the F_1-ATPase from thermophilic bacterium PS3 is accelerated by the chase-addition of excess ATP, J. Biol. Chem. 267 (1992) 4551–4556.
[29] J.M. Jault, W.S. Allison, Slow binding of ATP to noncatalytic nucleotide binding sites which accelerate catalysis is responsible for apparent negative cooperativity exhibited by the bovine mitochondrial F_1-ATPase, J. Biol. Chem. 268 (1993) 1558–1566.
[30] K. Yokoyama, E. Muneyuki, T. Amano, S. Mizutani, M. Yoshida, M. Ishida, S. Ohkuma, V-ATPase of *Thermus thermophilus* is inactivated during ATP hydrolysis but can synthesize ATP, J. Biol. Chem. 273 (1998) 20504–20510.
[31] A.E. Senior, S. Nadanaciva, J. Weber, The molecular mechanism of

ATP synthesis by F_1F_o-ATP synthase, Biochim. Biophys. Acta 1553 (2002) 188–211.

[32] J.-M. Zhou, P.D. Boyer, Evidence that energization of the chloroplast ATP synthase favors ATP formation at the tight binding catalytic site and increases the affinity for ADP at another catalytic site, J. Biol. Chem. 268 (1993) 1531–1538.

[33] E. Muneyuki, H. Noji, T. Amano, T. Masaike, M. Yoshida, F_oF_1-ATP synthase: general structural features of 'ATP-engine' and a problem on free energy transduction, Biochim. Biophys. Acta 1458 (2000) 467–481.